JOURNAL OF MATERIALS SCIENCE 32 (1997) 1075–1082

Grain boundary sliding during superplastic stretching of AA7475 cylindrical cups

M. G. ZELIN
Department of Chemical Engineering and Materials Science, University of California, Davis, CA 95616, USA

Topographic and microstructural examinations were performed at the deformed surface and also in the bulk superplastically stretched 7475 aluminum alloy cups. Sliding of grain groups at shear surfaces spaced at approximately four grain diameters was observed at strain level, $\varepsilon = 0.6$. The spacing between shear surfaces of such a cooperative grain boundary sliding (CGBS) decreases when the strain increases; it is approximately three grain diameters at $\varepsilon = 0.85$. The pattern of the CGBS surfaces is consistent with that predicted using slip line field theory. Long range correlated migration of sliding grain boundaries, the formation of dispersoid free zones and fibres have also been observed. These processes can be rationalized in terms of CGBS.

1. Introduction

The phenomenon of superplastic (SP) flow has been increasingly used in industrial applications. The advantages stemming from the use of SP deformation, such as extensive ductility reaching 1000%, low flow stress, etc. have motivated a significant interest in the understanding of the physical mechanism of SP flow. The studies so far performed have demonstrated that grain boundary sliding provides the dominant contribution to the total strain under optimal superplastic conditions [1, 2]. It was also shown that grain boundary sliding strongly affects the process of microstructural evolution, influencing the grain growth [3], cavity formation [4], and morphological changes in the phase distribution in materials with a microduplex type of microstructure [5]. The formation of precipitate free zones observed in dispersoid hardened materials, for instance, in Al alloys [6, 7] also depends on the extent of grain boundary sliding.

It was demonstrated recently [8, 9] that grain boundary sliding during SP deformation occurs in a co-operative manner, i.e., grain groups slide as an entity. Such a co-operative grain boundary sliding (CGBS) has been studied on different microstructural scales in a number of SP materials [10, 11]. It was particularly found [10, 11] that CGBS is accompanied by the rotation of grain groups and correlated grain boundary migration.

Most of the data on grain boundary sliding have been obtained on samples deformed in uniaxial tension. However, the metal forming processes used in commercial production involve more complex strain states, for example, bi-axial deformation in sheet forming.

Topographic studies of the deformed surface of superplastically bulged hemispherical AA7475 cups [12] highlighted similarities and differences in the progress of grain boundary sliding under bi-axial and uniaxial strain states. For instance, similarly to the case of uniaxial tension [11], the macroscopic pattern of surfaces of co-operative grain boundary sliding after bi-axial deformation was consistent with that predicted by slip line field theory. Fibre formation between grains moving apart was observed at these surfaces of CGBS. Similar fibres were found in uniaxially deformed AA7475 [13]. Such a process of fibre formation, which suggests an extremely high ductility of the material, was referred to as micro-superplasticity [14]. A significant out-of-sheet plane grain displacement observed after bi-axial stretching can serve as an example of the differences in grain boundary sliding occurring under bi-axial and uniaxial strain states. Note, that this previous study of grain boundary sliding in hemispherical cup formation only focused on a qualitative examination of the deformed surface.

In this paper, both deformed surface and microstructural evolution in the bulk have been studied in superplastically formed AA7475 cylindrical flat-bottomed cups. The emphasis in the surface examination was placed on studying the cooperative manner of grain boundary sliding. The effect of CGBS on micro-superplasticity and formation of dispersoid free zones was the object of microstructural studies performed in the bulk material.

2. Experimental procedure

7475 aluminum alloy sheets, 1.5 mm thick, with an average grain size, d, of approximately 10 μm were

* *Present address*: Concurrent Technologies Corporations 1450 Scalp Av., Johnstown, PA 15904, USA.

0022–2461

obtained from Kaiser Aluminum and Chemical, Co. The material exhibits typical superplastic behaviour in uniaxial tension at 515 °C and a strain rate of $\dot{\varepsilon} = 2 \times 10^{-4}\ s^{-1}$ [15]. The flat faces of square blanks, $50 \times 50\ mm^2$ were mechanically polished with a final polishing on 0.05 μm alumina. Marker lines were inscribed on the prepolished surface by using 3 μm diamond paste both parallel and perpendicular to the rolling direction.

Fig. 1a illustrates the geometry of a die assembly used to stretch cylindrical cups. Experiments were performed under the constant velocity of ram movement, $v = 4.3 \times 10^{-3}\ mm\ s^{-1}$. Fig. 1b demonstrates a dependence of actual strain rate as a function of the punch displacement. This dependence was derived assuming a uniform sheet thickness distribution (see Appendix). A nominal equivalent strain was also estimated based on the assumption on the uniform thickness. The optimal strain rate was within the interval of actual strain rate change.

Scanning electron microscopy (SEM) was used for both topographic examinations of the as-deformed surface of the bulged cups and for studying the microstructural evolution in the bulk. In the latter case, the sectioned cut cups were heat treated in order to obtain a better etching response [15]. The heat treatment included a soak at 400 °C for 5 min and water quenching with subsequent aging at 180 °C for 30 min. The mounted and mechanically polished specimens were etched by immersion in a 10% solution of H_3PO_4 in distilled water. The size of grain groups which slid as an entity, L, was measured on SEM microphotographs with an accuracy of ± 8.5 μm at a 90% confidence level and two hundred measurements. Chemical analysis was performed by using energy dispersive X-ray spectroscopy EDX and microprobe analysis. The beam spot resolution was 1 μm in both cases.

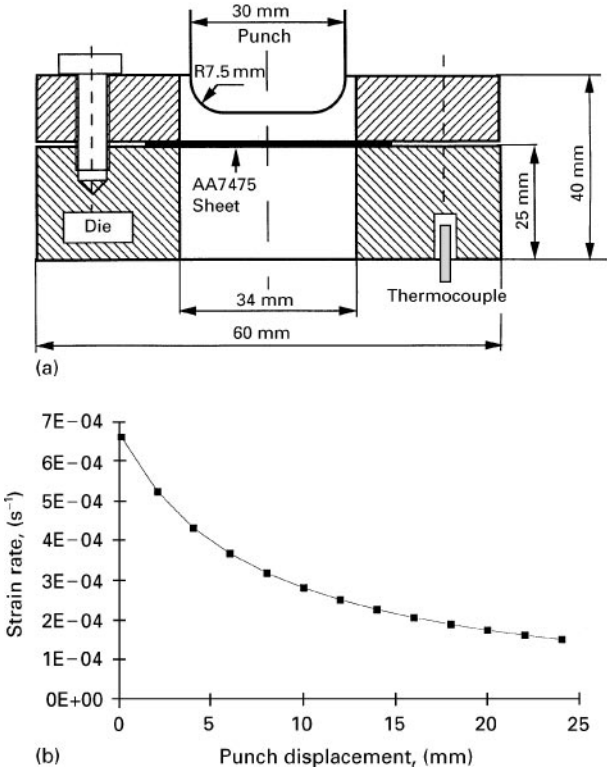

Figure 1 (a) – A schematic diagram of a die assembly used to stretch cylindrical cups. (b) – A dependence of actual strain rate changes as a function of the punch displacement.

3. Results

Fig. 2 shows the dependence of load, P, versus punch displacement. The rate of load increases only slightly while displacements are relatively small ($d < 8$ mm). Then the rate of load development increases significantly as the material is stretched over the punch radius. The rate of load development increases very gradually while the cup walls are being formed.

Fig. 3(a and b) show low magnification SEM micrographs taken from cups of different height (see insets). Contiguous chains of grain boundaries, which appear bright in secondary electron mode, are seen both in the top region and in the wall portion of the cups. The offset of marker lines at grain boundaries (Fig. 3(c and d) indicate that grain boundary sliding has occurred at the grain boundaries. The formation of surface steps, which appear bright because of extensive electron emission, is evident from Fig. 3(a–f). The fact that sliding grain boundaries form extended chains indicates the existence of a long-range correlation in grain boundary sliding. The movement of marker lines at grain boundaries of different grains are observed to be all in the same direction (for instance, between points A and B and points C and D in Fig. 3(e and f), respectively) also testifies to a co-operative manner of grain boundary sliding.

Co-operative grain boundary sliding results in significant displacements in the marker lines at sliding grain boundaries (Fig. 3(e and f)). The amount of marker line displacement increases with increasing strain. In some places it is comparable with the grain size, for example, near point C in Fig. 3f. At the same time, marker lines in between these sliding grain boundaries remain undisturbed (Fig. 4a). This indicates sliding of groups of grains situated between the CGBS surfaces. Such sliding grain blocks are clearly seen in the backscattered electron micrograph presented as Fig. 4b. Grain boundaries inside the sliding grain groups are outlined by precipitates (for instance, see the grain group designated by the letter K). The

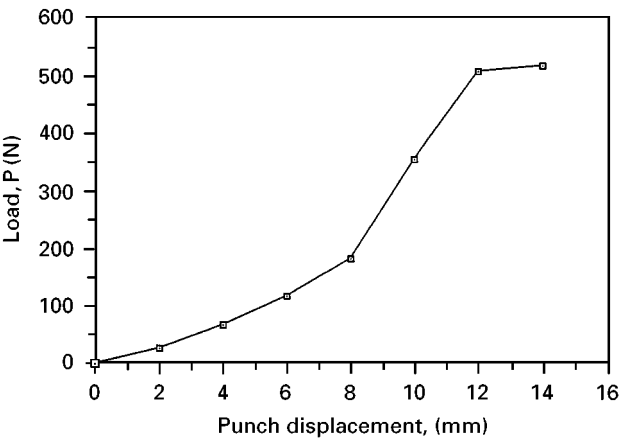

Figure 2 A dependence of the forming load, P, as a function of punch displacement.

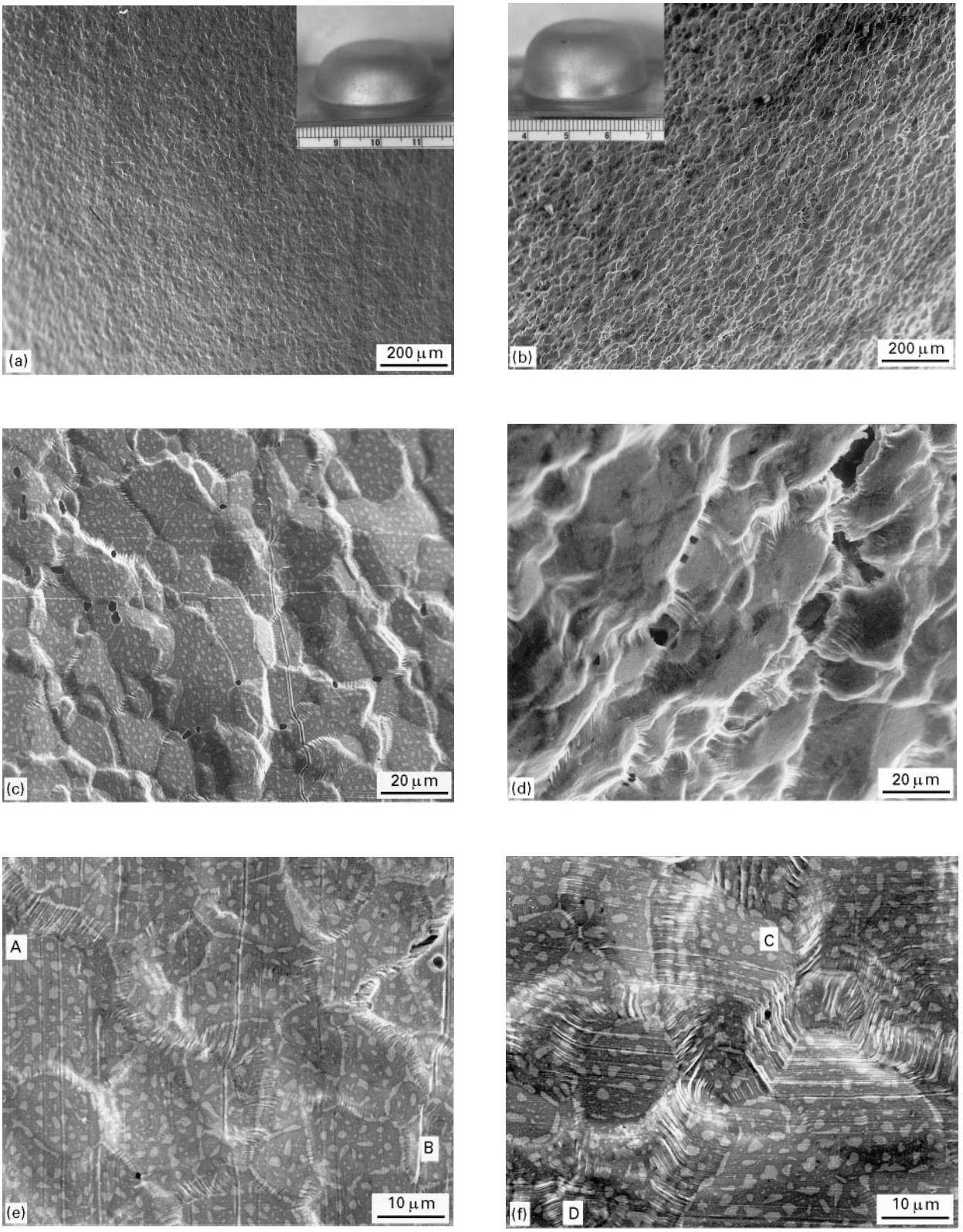

Figure 3 (a), (b) – Low magnification scanning electron micrographs taken from the prepolished surface of AA7475 sheet blanks superplastically stretched into cylindrical cups of different height (see insets). (c), (d) and (e), (f) illustrate the details of the deformed surface in the wall portion and in the top portion of the cups, respectively. The nominal equivalent plastic strain is $\varepsilon = 0.6$ (a, c, e) and $\varepsilon = 0.85$ (b, d, f).

length of undisturbed marker line segments, which reflects the size of sliding grain blocks, decreases when strain increases. Measurements of the length of the marker line segments (Fig. 5a) and of the size of grain blocks revealed due to grain boundary sliding (Fig. 5b) showed that an average size of the sliding grain groups, L, (see Fig. 5c) is approximately $L = 4d$ at a strain level $\varepsilon = 0.6$ and approximately $L = 3d$ at $\varepsilon = 0.85$. The size of sliding grain groups was measured between shear surfaces whose direction is indicated by arrows in Fig. 5d. Despite some ambiguities in the determination of the outlines of the sliding grain blocks, it more realistically reflects the real size of the sliding grain groups at higher strain levels than does the length of marker line segments. Numerous grain boundary displacements inside

sliding grain groups which have an accommodation character result in the breaking of marker lines at high strain levels, thereby complicating the determination of the real dimensions of the sliding grain groups.

Striations are observed at surfaces of CGBS (Fig. 3(c–f), Fig. 4 and Fig. 5c). These striations evolve into fibres when the amount of CGBS is significant. The directionality of the striations and fibres (arrowed in Fig. 6) is consistent with that of the GBS (see offset of marker lines in Fig. 3f, Fig. 5c and Fig. 6). EDX analysis from a fibre (arrowed in the inset given in Fig. 7b) indicates that there is a higher concentration of solute atoms (Fig. 7b) in comparison with that in the bulk (Fig. 7a). Precipitates elongated along the sliding direction are observed in the striated bands and the fibres. Microprobe analysis showed Zn and Cu as constituents of the precipitates.

The sliding of grain groups is accompanied by grain boundary migration. Steps seen in Fig. 8 (see also Fig. 6) are interim positions of migrating grain

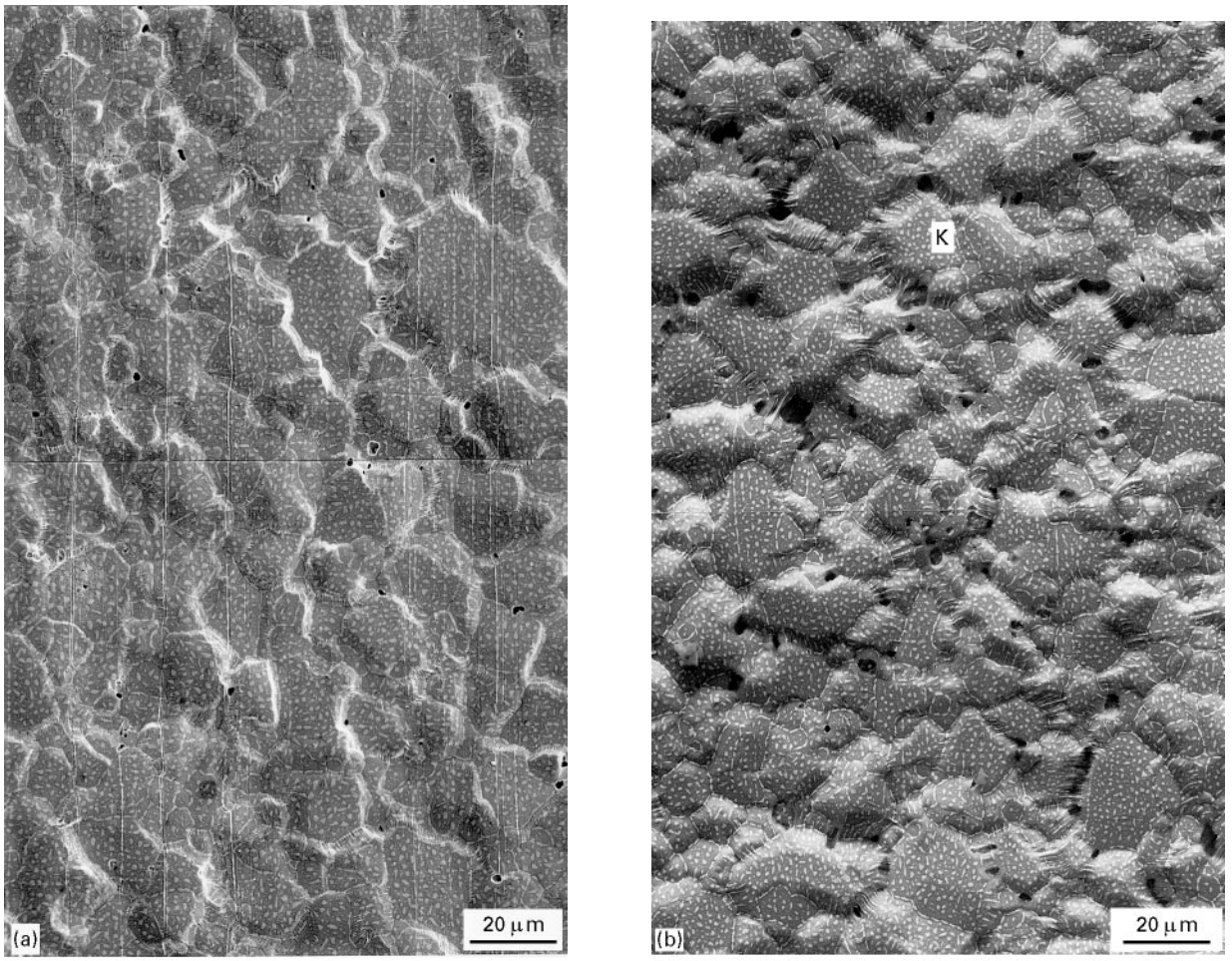

Figure 4 (a) Secondary electron and (b) backscatter electron micrographs illustrating group manner of GBS at $\varepsilon = 0.6$ (a) and $\varepsilon = 0.85$ (b). Grain boundaries outlined by precipitates are seen inside grain groups which slid as an entity (for instance, designated by a letter K in (b)).

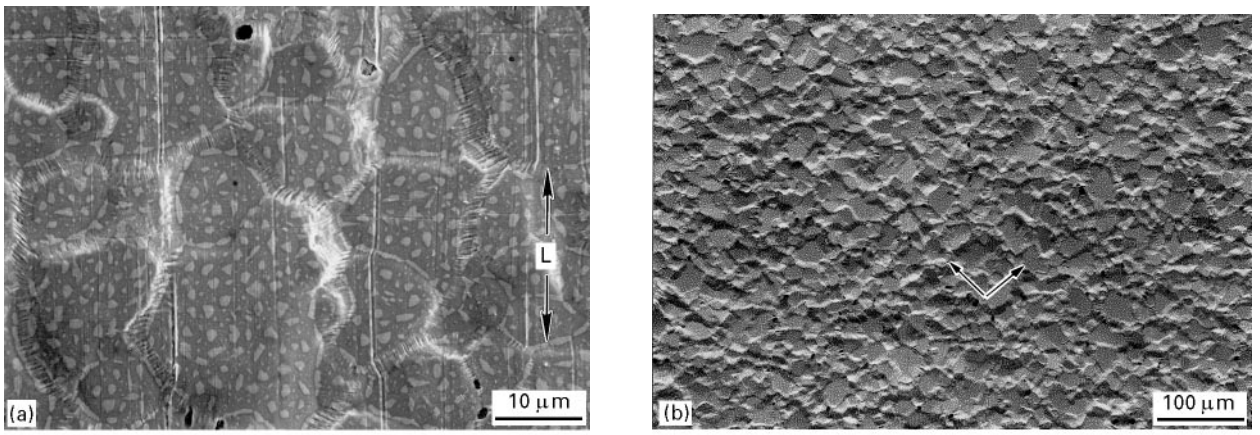

Figure 5 (a) Secondary and (b) backscatter electron micrographs taken from the top portion of a cylindrical cup and statistical distributions of sliding grain groups sizes at $\varepsilon = 0.6$ (c) and $\varepsilon = 0.85$ (d). Arrows in (b) indicate surfaces of CGBS. L is an average size of sliding grain groups.

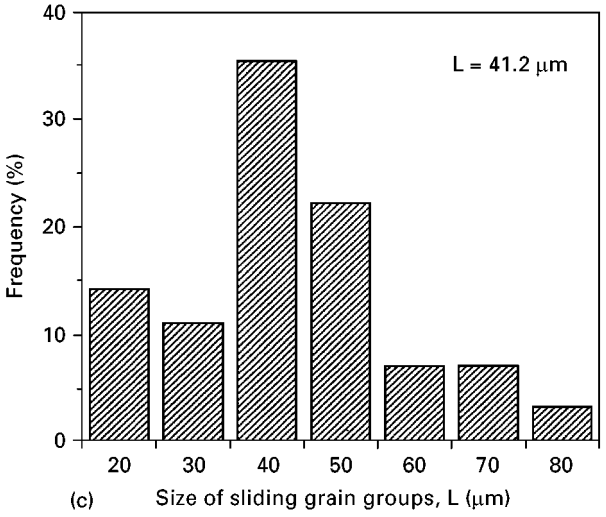

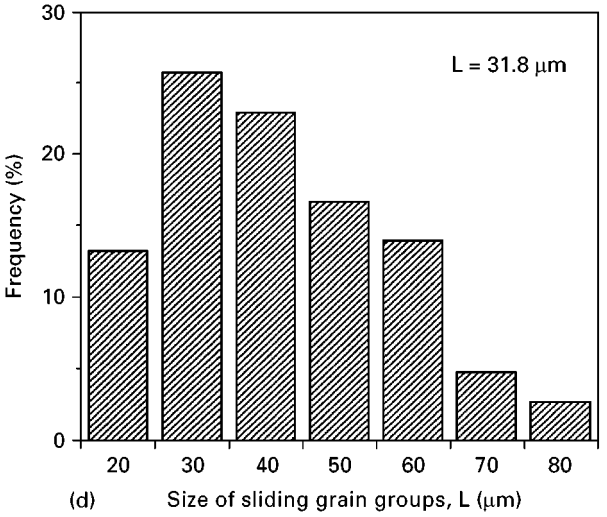

Figure 5 Continued.

Figure 6 An SEM micrograph showing fibres (arrowed) formed at grain boundaries as a result of CGBS in a superplastically stretched AA7475 cylindrical cup.

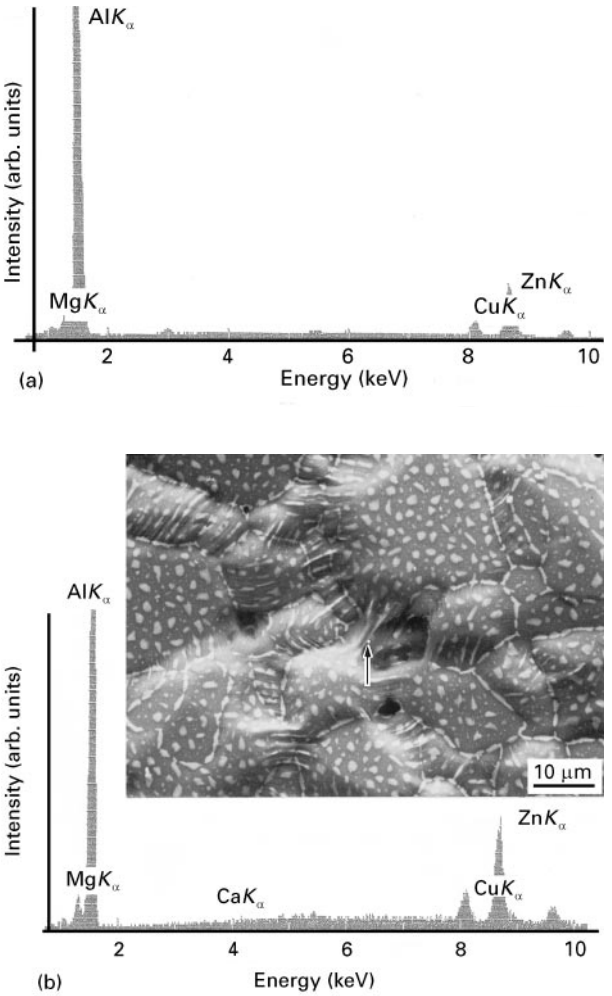

Figure 7 EDX spectrum from the bulk (a) and from a fibre (b) arrowed in the inset given in the upper corner in (b). Top region of a superplastically stretched AA7475 cylindrical cup.

boundaries. EDX analysis showed that the concentration of Cu, Zn, and Mg is often significantly higher in these regions than in the grain centre.

Similarly, the concentration of solute elements was higher in dispersoid free zones observed in the etched samples (Fig. 9). These zones form chains aligned with grain boundary surfaces oriented at 45–60° with respect to the sheet middle plane.

4. Discussion

The study of grain boundary sliding in the formation of cylindrical cups reported here was performed as a development of the previous study of grain boundary sliding in the formation of hemispherical cups [12], which, to the best of the author's knowledge was the first report on the occurrence of grain boundary sliding under a bi-axial strain state. In order to make it easier for the reader to compare results the data of both studies, are presented in a similar way.

The following features were observed in superplastically stretched cylindrical cups:

(i) Grain groups sliding as an entity
(ii) Correlated grain boundary migration
(iii) Dispersoid free zones
(iv) Fibres formed at the CGBS surfaces

Possible explanations for these observations are discussed below. Note that items (i), (ii) and (iv) were also observed in the case of the formation of hemispherical

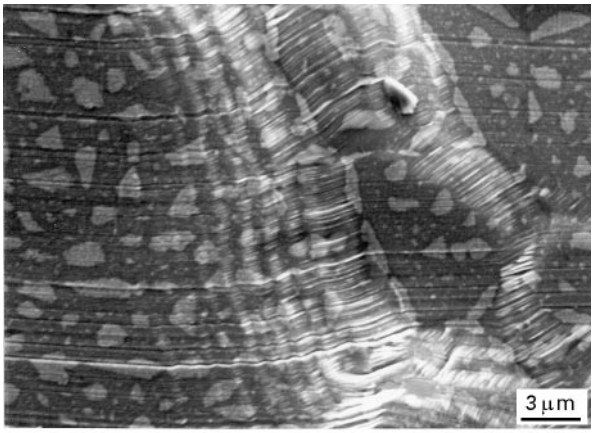

Figure 8 An SEM micrograph showing steps, which are interim positions of a migrating grain boundary in a superplastically stretched AA7475 cyclindrical cup.

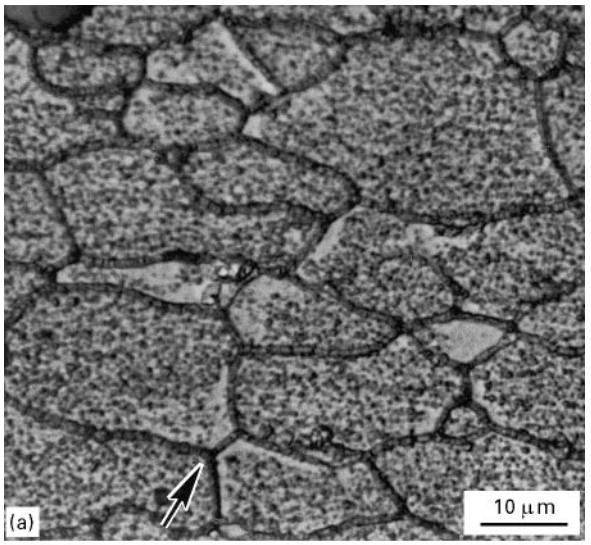

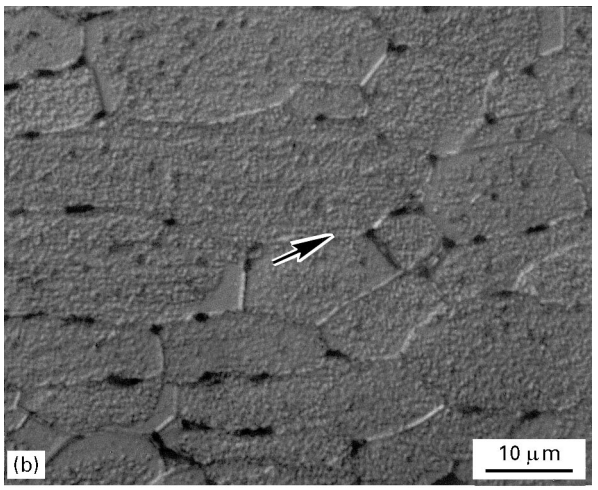

Figure 9 Dispersoid free zones in superplastically stretched AA7475 cylindrical cup. Optical microscopy; (b) using polarized light.

cups. This indicates that their general character is independant of the punch shape.

4.1. Cooperative grain boundary sliding

The process of CGBS occurs under the application of a shear stress. It could be expected that grain boundaries having an orientation close to the orientation of the maximum shear stress, are preferential sites for sliding. Consequently, a spatial pattern of sliding grain boundaries is consistent with that of surfaces of maximum shear stress.

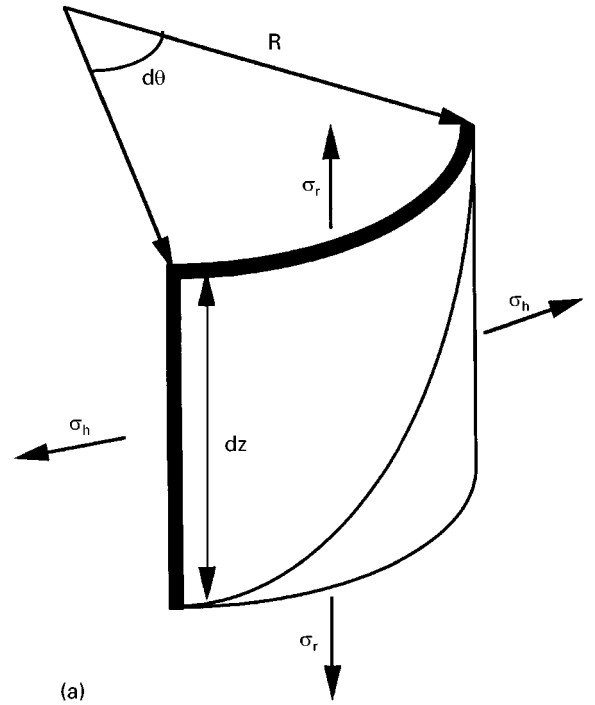

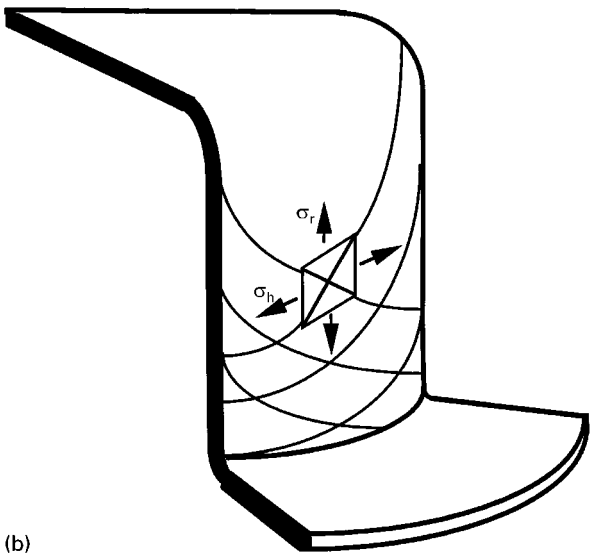

Figure 10 Schematic diagrams illustrating (a) the stress state in the wall portion of a cylindrical cup and (b) the pattern of CGBS surfaces.

The schematic diagram shown in Fig. 10a illustrates the stress state in the wall region of a cylindrical cup. Because of the small sheet thickness, the through thickness stress can be assumed to be equal to zero. The hoop stress, σ_h, and the meridian stress σ_r, are principal stresses in this case of a plane stress state in a body of rotational symmetry [16]. The maximum shear stress lies at 45° to the direction of the principal stress. Therefore, the orientation of the surfaces of maximum shear stress can be determined (see Fig. 9a) from the following equation [16]:

$$dz = \pm R\,d\theta \quad (1)$$

Integrating Equation 1 and expressing R and θ in Cartesian coordinates, one obtains:

$$z = \pm R(\tan^{-1}(y/x) + n\pi), \quad n = 0, 1, 2 \ldots \quad (2)$$
$$y^2 + x^2 = R^2$$

Equations 1 and 2 describe right and left helices (Fig. 9b) corresponding to the plus and minus signs, respectively. The fact that the CGBS surfaces of the helix shape were observed in the wall region (Fig. 3(a–d) and Fig. 4) support the developed analysis.

Quantitative data showing a decrease of spacing of shear surfaces with strain increase (Fig. 5(c and d)) are in agreement with qualitative observations made in hemispherical cups [12]. This trend is also consistent with observations performed in uniaxial tension [10, 11]. Note, that quantitative comparison of the contribution of grain boundary sliding to the total strain under bi-axial and uniaxial strain states is difficult to make. This requires knowledge of the geometrical coefficients [2], which have not been identified for the case of a bi-axial strain state.

4.2. Correlated grain boundary migration

A dislocation model of grain boundary sliding and migration suggests [17, 18] that parallel and normal components of the Burgers' vector of grain boundary dislocations results in the grain shear and grain boundary migration, respectively. From this, migration of grain boundaries forming CGBS surfaces can be expected. A long range correlation in the grain shear caused by the co-operative manner of grain boundary sliding results in the correlated manner of grain boundary migration.

Observations of steps, which are interim positions of a migrating grain boundary, predominantly at the sliding grain boundaries supports the above explanation. Results of the chemical analysis showed that the solute atom concentration is often higher in the vicinity of sliding/migrating grain boundaries in comparison to that in the grain centre. This indicates that grain boundary migration is accompanied by the process of dissolution of disperse particles and results in the formation of dispersoid free zones.

4.3. Dispersoid free zones

The formation of DFZ in dispersoid hardened materials is well documented. A number of reasons for the formation of DFZ have been considered including diffusional creep [19], dissolution of dispersoids during cooling [20], and grain boundary migration [21]. The detailed analysis of experimental results, which agree with current observations, indicate that the origin of DFZ can be attributed to grain boundary migration [6]. To avoid repetition, only facts that did not receive appropriate attention in previous studies [6, 7, 22, 23] are emphasized here, specifically: (i) DFZ form quite long chains and (ii) there is a certain pattern in DFZ that is similar to that formed by CGBS surfaces. The last fact is less obvious at small strains (Fig. 9), but two intersecting systems of DFZ are clearly seen after large superplastic strains [6, 7].

Both these facts can be explained from the point of view of co-operative grain boundary sliding and migration. The existence of long range correlation in the migration of sliding boundaries results in the formation of elongated chains of DFZ. Their orientation is consistent with that of CGBS surfaces, which form the pattern discussed above. Backofen *et al.* [24] have also reported that the pattern of DFZ is similar to that of striation bands, which outline CGBS surfaces. These striations evolve into fibres when the amount of sliding increases.

4.4. Fibre formation

Similarly to the case of forming a hemispherical cup [12], fibres at the surface of cylindrical cups are formed between grains separating due to CGBS. The chemical composition of the fibres is close to that of the bulk material with an increased concentration of solute atoms in some instances. It has been shown [25] that fibre formation is very sensitive to the environment. Fibres were observed only if the surface on which they had been formed was exposed to the air.

Incipient melting of low melting temperature phases was suggested as one of the possible mechanisms for fibre formation [26]. However, the fact that the phenomenon of microsuperplasticity has been observed at temperatures as low as 200 °C [25] does not support this assumption.

It is difficult to explain fibre formation from the point of view of mechanisms operating during microstructural superplastic flow, i.e., grain boundary sliding, diffusion creep and dislocation deformation [1]. The fibre diameter is much less than an average grain size in the bulk material, which rules out grain boundary sliding of the bulk grains from the list of possible explanations. The rate of classical mechanisms of diffusion creep are too low to explain the tremendous deformations which the material underwent in order to form the fibres in a relatively short period of time, particularly during failure [14, 25]. It is also improbable to suggest an active diffusion creep in the case of low temperatures. Observations performed at large magnifications showed that the fibres have non-uniform thickness. This might be interpreted in terms of the operation of several necks in a fibre gauge. This fact can also be related to the formation of surface steps due to the operation of a dislocation deformation. However, if the last assumption is correct, it is not clear how oxidation promotes dislocation activity. The fact that microsuperplasticity is sensitive to oxygen might be indicative of superplastic flow of phase transformation type [27].

5. Summary

A study of the deformed surface and microstructure in the bulk of superplastically stretched AA7475 cylindrical cups showed the following:

1. Grain boundary sliding occurs in a co-operative manner, i.e., grain groups slide as an entity. The

pattern of macroscopic surfaces at which sliding of grain blocks takes place is consistent with that predicted by use of the slip line field theory.
2. The spacing of the shear surfaces is approximately four grain diameters at a strain level $\varepsilon = 0.6$ and approximately three grain diameters at $\varepsilon = 0.85$.
3. The observed correlated migration of sliding grain boundaries and the formation of dispersoid free zones and fibres can be attributed to the operation of a co-operated grain boundary sliding. The possible explanations for the above phenomena have been discussed.

Acknowledgement

This work was supported by a grant (Number DMR-93-00217) from the U.S. National Science Foundation. The author wishes to thank Prof. A. K. Mukherjee for his valuable discussion and support, Dr. A. T. Male for his comments and Dr. H. S. Yang for providing the material.

Appendix

The actual strain rate changes as a function of the punch displacement can be easily estimated for the case of a cylindrical punch without considering effect of the radius at the top. For this simple punch geometry plane strain conditions can be assumed in the wall region. Because of the constraint from the punch [28], hoop strain is equal to zero, and the through thickness strain, ε_s, is equal to the meridian strain, ε_m. The through thickness strain can be defined as:

$$\varepsilon_s = -\ln s/s_0 \quad \text{A1}$$

or because of volume constancy, $A\,s = \text{constant}$,

$$\varepsilon_s = \ln A/A_0 \quad \text{A2}$$

Here, s and s_0 are current and initial thickness, and A and A_0 are current and initial surface area of the deformed sheet, respectively.
Then, through thickness strain rate is defined as:

$$\dot{\varepsilon}_s = \dot{A}/A \quad \text{A3}$$

The surface area is determined as:

$$A = 2\pi Rh + \pi R^2 \quad \text{A4}$$

and Equation A2 and Equation A3 become, respectively

$$\varepsilon_s = \ln(2h/R + 1) \quad \text{A5}$$

$$\dot{\varepsilon}_s = 2v/(2h + R) \quad \text{A6}$$

where h and $v = \dot{h}$ are punch displacement and velocity of punch displacement, respectively. Since for the plane strain:

$$\varepsilon = 2/(3)^{0.5}\,\varepsilon_s \quad \text{A7}$$

Equations A5 and A6 can be written in the following form:

$$\varepsilon = 2/(3)^{0.5} \ln(2h/R + 1) \quad \text{A8}$$

$$\dot{\varepsilon} = 2/(3)^{0.5}\, v/(2h + R) \quad \text{A9}$$

The nominal equivalent strain can be estimated according to Equation A8 if the dome height is known. The actual strain rate decreases while the punch displacement increases (Fig. 2b) when the velocity of punch displacement is a constant. However, the actual strain rate is varying in the range, which is close to the optimum superplastic strain rate.

References

1. J. PILLING and N. RIDLEY, "Superplasticity in Crystalline Solids" (The Institute of Metals, London, 1989) p. 240.
2. T. G. LANGDON, *Metals Forum* **4** (1981) 14.
3. D. S. WILKINSON and C. H. CACERES, *Acta Metall.* **32** (1984) 1335.
4. A. H. CHOKSHI, A. K. MUKHERJEE and T. G. LANGDON, *Mater. Sci. Engng* **R10** (1993) 237.
5. H. S. YANG, M. G. ZELIN, R. Z. VALIEV and A. K. MUKHERJEE, *Scr. Met. Mater.* **26** (1992) 1707.
6. U. KOCH, in "Superplasticity in Aerospace I", edited by H. C. Heikken and T. R. McNelley (The Metallurgical Society, Warrendalle, PA, 1988) p. 115.
7. W. CAO, X. LU, A. F. SPRECHER and H. CONRAD, in "Superplasticity in Aerospace II", edited by H. C. Heikken and T. R. McNelley (The Metallurgical Society, Warrendalle, PA, 1990) p. 269.
8. M. G. ZELIN and A. K. MUKHERJEE, *Phil. Mag.* **68** (1993) 1183.
9. V. V. ASTANIN, O. A. KAIBYSHEV and S. N. FAIZOVA, *Acta Met Mater.* **42** (1994) 2617.
10. M. G. ZELIN and A. K. MUKHERJEE, *Mater. Sci. Forum* **170–172** (1994) 29.
11. *Idem., Acta Met Mater.* **43** (1995) 2359.
12. M. G. ZELIN, *J. Mater. Sci.* **31** (1996) 843.
13. A. VARLOTEAUX, J. J. BLANDIN and M. SUERY, *Mater. Sci. and Technol.* **5** (1989) 1109.
14. W. J. D. SHAW, *Mater Lett.* **4** (1985) 1.
15. H. S. YANG, Kaiser Aluminum & Chemical Co., internal report (1994).
16. A. D. TOMLYENOV, "Theory of Plastic Deformation of Metals" (Metallurgy, Moscow, 1972) p. 232.
17. R. C. POND, D. A. SMITH and P. W. J. SOUTHERDREN, *Phil. Mag.* **A37** (1978) 27.
18. A. H. KING, *Acta Metall.* **22** (1974) 567.
19. T. B. GIBBONS, *Metal Sci. J.* **6** (1972) 13.
20. P. N. T. UNWIN, G. W. LORIMER and R. B. NICHOLSON, *Acta Metall.* **17** (1969) 1363.
21. M. F. ASHBY and R. M. A. CENTAMORE, *ibid.* **16** (1968) 1081.
22. U. KOCH, W. BUNK and P.-J. WINKLER, in "Superplasticity in Advanced Materials", edited by S. Hori, M. Tokizane and N. Furushiro (The Japan Society for Research on Superplasticity, Osaka, 1991) p. 57.
23. J. A. WERT and A. VARLOTEAUX, in "Aluminum Alloys, their Physical and Mechanical Properties, II", edited by E. A. Starke and T. H. Sanders (University of Virginia, Charlottsville, VA, 1986) p. 1255.
24. W. A. BACKOFEN, G. S. MURTY and S. W. ZEHR, *Trans. Metall. Soc.* AIME **242** (1968) 329.
25. S. F. CLAEYS, J.W. JONES and J. E. ALLISON, in "Dispersion Strengthened Aluminum Alloys", edited by Y.-W. Kim and W. M. Griffith (The Minerals, Metals & Materials Society, Warrendale, PA, 1988) p. 323.
26. T. HIKOSAKA, T. IMAI, T. G. NIEH and J. WADSWORTH, *Scripta Metall. Mater.* **31** (1994) 1181.
27. J. WADSWORTH and O. D. SHERBY, *Mater. Sci. and Technol.* **1** (1985) 925.
28. J. M. ALEXANDER, *Metall. Reviews* **5** (1960) 349.

Received 7 September 1995
and accepted 15 January 1996